International Journal of
Molecular Sciences

MDPI

Article

Low-Dose Empagliflozin Improves Systolic Heart Function after Myocardial Infarction in Rats: Regulation of MMP9, NHE1, and SERCA2a

Jana Goerg [1,2], Manuela Sommerfeld [1,2], Bettina Greiner [1,2], Dilyara Lauer [1], Yasemin Seckin [1,3], Alexander Kulikov [4], Dmitry Ivkin [5], Ulrich Kintscher [1,2], Sergey Okovityi [5] and Elena Kaschina [1,2,*]

1 Charité-Universitätsmedizin Berlin, Corporate Member of Freie Universität Berlin and Humboldt-Universität zu Berlin, Institute of Pharmacology, Center for Cardiovascular Research (CCR), 10115 Berlin, Germany; jana-catherine.goerg@charite.de (J.G.); manuela.sommerfeld@charite.de (M.S.); bettina.greiner@charite.de (B.G.); dilyara.lauer@nuvisan.com (D.L.); yaseminseckin1992@gmx.de (Y.S.); ulrich.kintscher@charite.de (U.K.)
2 DZHK (German Centre for Cardiovascular Research), Partner Site Berlin, 10115 Berlin, Germany
3 Department of Biotechnology, University of Applied Science, 13353 Berlin, Germany
4 Pavlov First Saint-Petersburg State Medical University, 197022 Saint Petersburg, Russia; fd1med@mail.ru
5 Saint-Petersburg State Chemical-Pharmaceutical University, 197376 Saint Petersburg, Russia; dmitry.ivkin@pharminnotech.com (D.I.); Sergey.Okovity@pharminnotech.com (S.O.)
* Correspondence: elena.kaschina@charite.de; Tel.: +49-30-450-525-024

Abstract: The effects of the selective sodium-glucose cotransporter 2 (SGLT2) inhibitor empagliflozin in low dose on cardiac function were investigated in normoglycemic rats. Cardiac parameters were measured by intracardiac catheterization 30 min after intravenous application of empagliflozin to healthy animals. Empagliflozin increased the ventricular systolic pressure, mean pressure, and the max dP/dt ($p < 0.05$). Similarly, treatment with empagliflozin (1 mg/kg, p.o.) for one week increased the cardiac output, stroke volume, and fractional shortening ($p < 0.05$). Myocardial infarction (MI) was induced by ligation of the left coronary artery. On day 7 post MI, empagliflozin (1 mg/kg, p.o.) improved the systolic heart function as shown by the global longitudinal strain ($-21.0 \pm 1.1\%$ vs. $-16.6 \pm 0.7\%$ in vehicle; $p < 0.05$). In peri-infarct tissues, empagliflozin decreased the protein expression of matrix metalloproteinase 9 (MMP9) and favorably regulated the cardiac transporters sarco/endoplasmic reticulum Ca^{2+}-ATPase (SERCA2a) and sodium hydrogen exchanger 1 (NHE1). In H9c2 cardiac cells, empagliflozin decreased the MMP2,9 activity and prevented apoptosis. Empagliflozin did not alter the arterial stiffness, blood pressure, markers of fibrosis, and necroptosis. Altogether, short-term treatment with low-dose empagliflozin increased the cardiac contractility in normoglycemic rats and improved the systolic heart function in the early phase after MI. These effects are attributed to a down-regulation of MMP9 and NHE1, and an up-regulation of SERCA2a. This study is of clinical importance because it suggests that a low-dose treatment option with empagliflozin may improve cardiovascular outcomes post-MI. Down-regulation of MMPs could be relevant to many remodeling processes including cancer disease.

Keywords: empagliflozin; myocardial infarction; MMP9; NHE1; SERCA2a

Citation: Goerg, J.; Sommerfeld, M.; Greiner, B.; Lauer, D.; Seckin, Y.; Kulikov, A.; Ivkin, D.; Kintscher, U.; Okovityi, S.; Kaschina, E. Low-Dose Empagliflozin Improves Systolic Heart Function after Myocardial Infarction in Rats: Regulation of MMP9, NHE1, and SERCA2a. *Int. J. Mol. Sci.* **2021**, *22*, 5437. https://doi.org/10.3390/ijms22115437

Academic Editor: Łukasz Bułdak

Received: 21 April 2021
Accepted: 18 May 2021
Published: 21 May 2021

1. Introduction

Recent clinical studies demonstrated favorable cardiovascular effects of the antidiabetic drugs from the sodium-glucose cotransporter 2 (SGLT2) inhibitor class, including a reduction of cardiovascular death, non-fatal myocardial infarction (MI), heart failure, and non-fatal stroke, as well as all-cause mortality [1–6]. In experimental models, cardiac contractility was improved in heart failure with preserved and reduced ejection fractions [7–11], in ischemia/reperfusion [12], MI models [13–17], and diabetic cardiomyopathy [18]. Recently, the antiarrhythmic properties of SGLT2 inhibitors were shown in the ischemia-reperfusion model [19] and atrial fibrillation [20].

The glucose-lowering effect of SGLT2 inhibitors is a result of reduced glucose reabsorption from the primary urine due to the SGLT2 cotransporter inhibition in the proximal tubule of the kidney [21]. However, the exact cardio-protective mechanism of action is still unclear—especially since SGLT2 receptors are not expressed in the heart [22,23]. Several favorable effects of SGLT2 inhibitors such as increased diuresis [24], decreased arterial stiffness [25], weight and blood pressure reduction [1,26], and other cardiac benefits [27] contribute to positive outcomes in heart failure. The cardioprotective effects were also attributed to the modification of the cardiac metabolome and anti-oxidants [13], increased energy production from glucose, ketone bodies and fatty acid oxidation [10,28], anti-inflammation [29], and improved myocardial oxidative phosphorylation [30]. Moreover, empagliflozin reduced Ca^{2+}/calmodulin-dependent kinase II (CaMKII)-activity and CaMKII-dependent SR Ca^{2+} leak in ventricular myocytes [31].

It has been hypothesized that the selective SGLT2 inhibitor empagliflozin (Empa) may directly interfere with the cardiac sodium hydrogen exchanger 1 (NHE1) [32]. Modulation of NHE1 activity by Empa, in turn, decreased the cytosolic sodium and calcium levels while increasing the myocytes mitochondrial calcium concentration [32]. In an isolated heart, a delayed ischemic contracture onset by Empa was associated with NHE1 inhibition [33].

Nevertheless, the regulation of NHE1 and related cardiac pumps such as sodium bicarbonate cotransporter 1 (NBCe1), Na^+/Ca^{2+} exchanger (NCX), sarco/endoplasmic reticulum Ca^{2+}-ATPase (SERCA)2a in cardiac tissues after MI have not been tested until now. SERCA2a is the primary cardiac isoform regulating intracellular Ca^{2+}homeostasis. Its downregulation in heart failure leads to a loss of cardiac contractility whereas increased expression of SERCA2a improves contractility [34]. Down-regulation of SERCA2a after MI in rats was linked with diastolic dysfunction [35]. It was also assumed that a compensatory increase in NCX compensates for the reduced SERCA2a activity [34]. NCX is the main Ca^{2+} extrusion mechanism of the cardiac myocyte which is involved in the regulation of cytosolic Ca^{2+} concentration, repolarization, and contractility [36]. Its increased activity has been identified as a mechanism promoting heart failure, cardiac ischemia, and arrhythmia [36]. NBCe1 contributes to the control of intracellular pH in cardiomyocytes [37] and its blockade may reduce ischemic Na+ overload [38].

Moreover, a relationship between NHE1 and matrix metalloproteinase 9 (MMP9) might also exist in the heart; as well as neuronal tissues where MMP9 activity is dependent upon the expression and activation of NHE1 [39]. Therefore, Empa might contribute to the regulation of MMPs in the heart directly or via NHE1. We tested this hypothesis in an experimental MI model. We also designed the present study to assess the short-term effects of the treatment with the selective SGLT2 inhibitor Empa in normoglycemic rats, 1 week after MI. In contrast to previous experiments where the dose of Empa ranged from 20 to 30 mg/kg [14,15,40], we used a lower dose of 1 mg/kg. This dose was based on our preliminary cell culture experiments and was successful in our previous experimental heart failure study [11].

2. Results

2.1. Short-Term Hemodynamic Effects of Empagliflozin

In the control healthy rats, Empa (1 mg/kg, i.v. bolus) increased the left ventricular maximal pressure (110.2 ± 5.3 mmHg vs. 86.1 ± 7.1 mmHg; $p < 0.05$) and the mean pressure (53.8 ± 4.7 mmHg vs. 36.0 ± 4.8 mmHg; $p < 0.05$) as compared to vehicle (Figure 1A,B). In addition, the max dP/dt (5685.6 ± 545.9 vs. 8446.0 ± 742.5; $p < 0.05$; Figure 1C) and Tau (0.01056 ± 0.00109 vs. 0.01549 ± 0.0011; $p < 0.01$) were increased from the initial value to 30 min after Empa application. Moreover, dP/dt min was decreased by tendency. The heart rate slightly decreased 30 min after application in vehicle and Empa groups.

The aortic stiffness parameters: augmentation index, pulse pressure (Pp) (Figure 1D), and second systolic peak pressure (P2) were increased to a similar extent in Empa and vehicle groups.

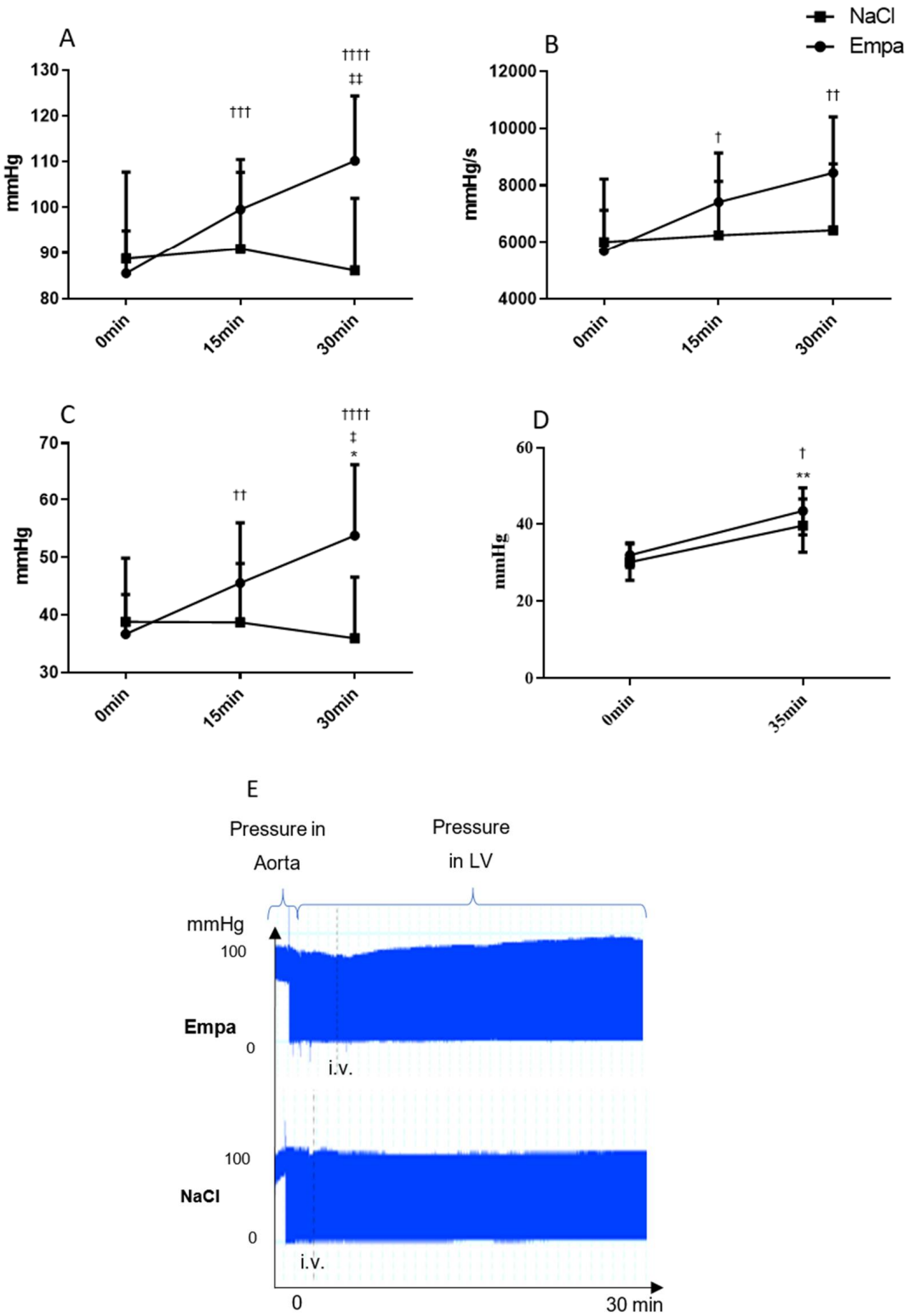

Figure 1. Hemodynamic parameters measured in the left ventricle by a cardiac catheter at baseline (0 min), 15 min, and 30 min after injecting NaCl or empagliflozin (Empa) (1 mg/kg/bw). Pressure mmHg (*x*-axis) at different time of measurements (*y*-axis). (**A**) Left ventricular maximal pressure (max pressure), * $P < 0.05$ Empa vs. NaCl 30 min; ††† $P < 0.001$, †††† $P < 0.0001$ vs. 0 min Empa, ‡‡ $P < 0.01$ vs. 15 min Empa. (B) Maximal rate of rise of left ventricular pressure (max dP/dt); † $P < 0.05$, †† P < 0.1 vs. 0 min Empa. (C) Mean Pressure; * $P < 0.05$ Empa 30 min vs. NaCl 30 min, †† $P < 0.01$, †††† $P < 0.0001$ vs. 0 min Empa, ‡ $P < 0.05$ vs. 15 min Empa. (D). Pulse pressure † $P < 0.05$, vs. 0 min Empa; ** $P < 0.05$ vs. 0 min NaCl. (E) Aortal and left ventricular pressure traces after Empa or NaCl administration, mean ± SD.

2.2. Hemodynamic Evaluation One Week after Myocardial Infarction

Post infarct mortality was 35%. The animals died within the first 24 h after MI. Hemodynamic parameters obtained one week after MI/sham operation are presented in Figure 2 and Table 1. Mean EF, FS and GLS were equal in all treatment groups at the start of the treatment. One week after MI, Empa protected against the impairment of systolic heart function as demonstrated by an improved global longitudinal strain (GLS) (MI + Empa; $-20.99 \pm 3.21\%$ vs. MI + Veh; $-16.64 \pm 1.61\%$; $p < 0.05$) compared to vehicle (Figure 2A). Ejection fraction slightly increased in treated group vs. vehicle (Figure 2B). The E/A ratio tended to decrease. Blood pressure, heart rate, and arterial augmentation index were not modified by the treatment. Sham-operated animals treated with Empa showed an increase in stroke volume (274.8 ± 27.6 µL vs. 209.5 ± 22.77 µL; $p < 0.01$), fractional shortening ($21.21 \pm 1.58\%$ vs. $16.01 \pm 3.54\%$; $p < 0.05$), and cardiac output (105.8 ± 7.9 mL/min vs 86.6 ± 10.2 mL/min; $p < 0.05$) in comparison to sham treated with vehicle.

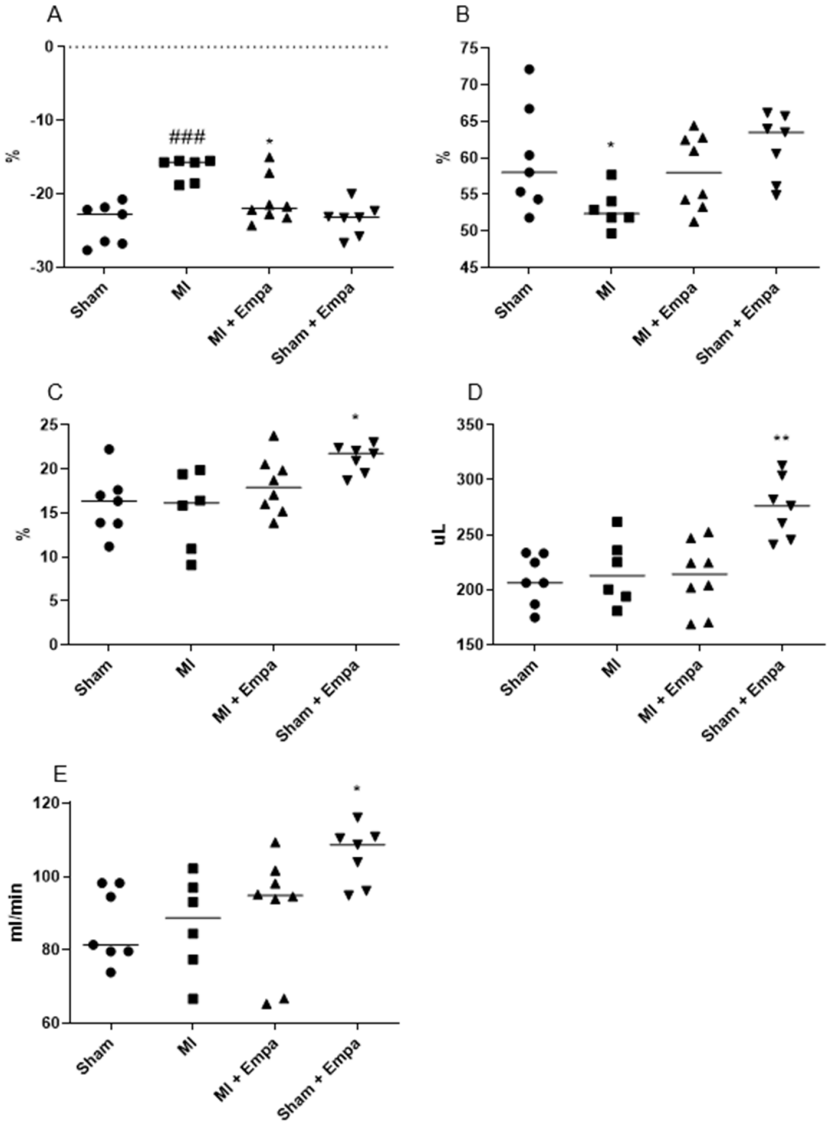

Figure 2. Hemodynamic parameters measured by Transthoracic Doppler Echocardiography 7 days after myocardial infarction (MI). (**A**) Global longitudinal strain (GLS); * $P < 0.05$ vs. MI, ### $P < 0.001$ vs. sham; 2-way Anova. (**B**) Ejection fraction (EF); * $P < 0.05$ vs. MI; unpaired t-test. (**C**) Fractional shortening (FS); *y*-axis: sham operation, MI vehicle, MI treated with Empa, sham operation treated with Empa; * $P < 0.05$ vs. sham; 2-way Anova. (**D**) Stroke volume (SV); ** $P < 0.01$ vs. sham, 2-way Anova. (**E**) Cardiac output; * $P < 0.05$ vs sham; 2-way Anova. (n = 7–8), mean ± SEM.

Table 1. Hemodynamic parameters measured 7 days after myocardial infarction via echocardiography.

	Sham	Sham + Empa	MI + Vehicle	MI + Empa
Heart rate (bpm)	413 ± 21	386 ± 14	401 ± 19	426 ± 34
EF (%)	59.9 ± 7.2	61.6 ± 4.5	53.0 ± 2.7	58.0 ± 5.1
GLS (%)	−24.1 ± 2.8	−23.5 ± 2.2	−16.6 ± 1.6 †††	−21.9 ± 3.2 *
FS (%)	16.0 ± 3.5	21.2 ± 1.6 †	15.3 ± 4.4	18.1 ± 3.2
SV (uL)	209.5 ± 22.8	274.8 ± 27.6 ††	216.4 ± 30.2	211.7 ± 31.5
CO (mL/min)	86.5 ± 10.2	105.8 ± 7.9 †	86.8 ± 13.3	90.6 ± 16
LVIDd (mm)	6.6 ± 0.3	7.3 ± 0.2	6.9 ± 0.5	6.9 ± 0.6
LVIDs (mm)	3.8 ± 0.6	3.8 ± 0.6	3.6 ± 0.7	3.7 ± 0.9
E/A Ratio	1.71 ± 0.24	1.58 ± 0.14	1.84 ± 0.31	1.69 ± 0.25
IVRT (mm/s)	0.05120 ± 0.00743	0.05123 ± 0.00508	0.05715 ± 0.00841	0.04585 ± 0.00810
IVCT (mm/s)	0.04754 ± 0.01319	0.04417 ± 0.01057	0.04616 ± 0.00893	0.03804 ± 0.00965

* $P < 0.05$ vs. vehicle treated animals; † $p < 0.05$ vs. sham, †† $p < 0.01$ vs. sham, ††† $p < 0.001$ vs. sham. Heart rate (bpm—beats per minute). EF—ejection fraction; GLS—global longitudinal strain; FS—fractional shortening; SV—stroke volume; CO—cardiac output; LVIDd—end-diastolic left ventricular internal diameter; LVIDs—end-systolic left ventricular internal diameter; E/A ratio—ratio of early to late mitral inflow diastolic velocities. IVRT—isovolumic relaxation time; IVCT—isovolumic contraction time (n = 6–8), mean ± SEM.

One week post-MI, Empa treated MI animals had a lower weight gain compared to vehicle (12.0 ± 9.9 g vs. 32.0 ± 13.6 g; $p < 0.05$). Heart/body weight index increased both in vehicle MI ($p < 0.05$) and Empa MI group ($p < 0.01$). There was no significant difference between the groups in the blood and urine glucose levels. Empa increased the urine glucose excretion in the sham group only by tendency (data not shown).

2.3. Regulation of Cardiac Transporters

The protein expression of cardiac transporters (NHE1, NBC, NCX, and SERCA2a) was examined in the peri-infarct zone of the left ventricle (Figure 3A,B). NHE1 was significantly down-regulated (2-fold, $p < 0.05$) by Empa post-MI compared to MI + vehicle, and decreased by the tendency in the Empa treated sham group compared to sham (1.4-fold). In the heart, NHE1 was localized at the plasma membrane of myocytes and transverse tubules as shown in the histological section of a rat heart (Figure 4A). Empa treated rats expressed less NHE1 compared to vehicle (Figure 4A(b)). In addition, in H9c2 cell line, Empa (5 µM) down-regulated NHE1 (110 kDa) (Figure 5).

The expression of NCX was increased after MI by tendency but not affected by Empa (Figure 3A,B). NBC1 (130 kDa) was not changed, whereas the 60 kDa form was upregulated (1.5-fold, $p < 0.05$) in the MI Empa group. SERCA2a was decreased (1.4-fold) post-MI, and its decrease was ameliorated by Empa ($p < 0.05$). After i.v. application of Empa in short-term experiments, cardiac expression of SERCA2a was 1.2-fold lower compared to the NaCl group. Immunohistological stain showed that SERCA2a was highly expressed in healthy cardiomyocytes co-localizing with sarcomere structures (Figure 4B(a)). Less SERCA2a staining was found in the MI group (Figure 4B(b)) and more in the Empa group (Figure 4B(c)).

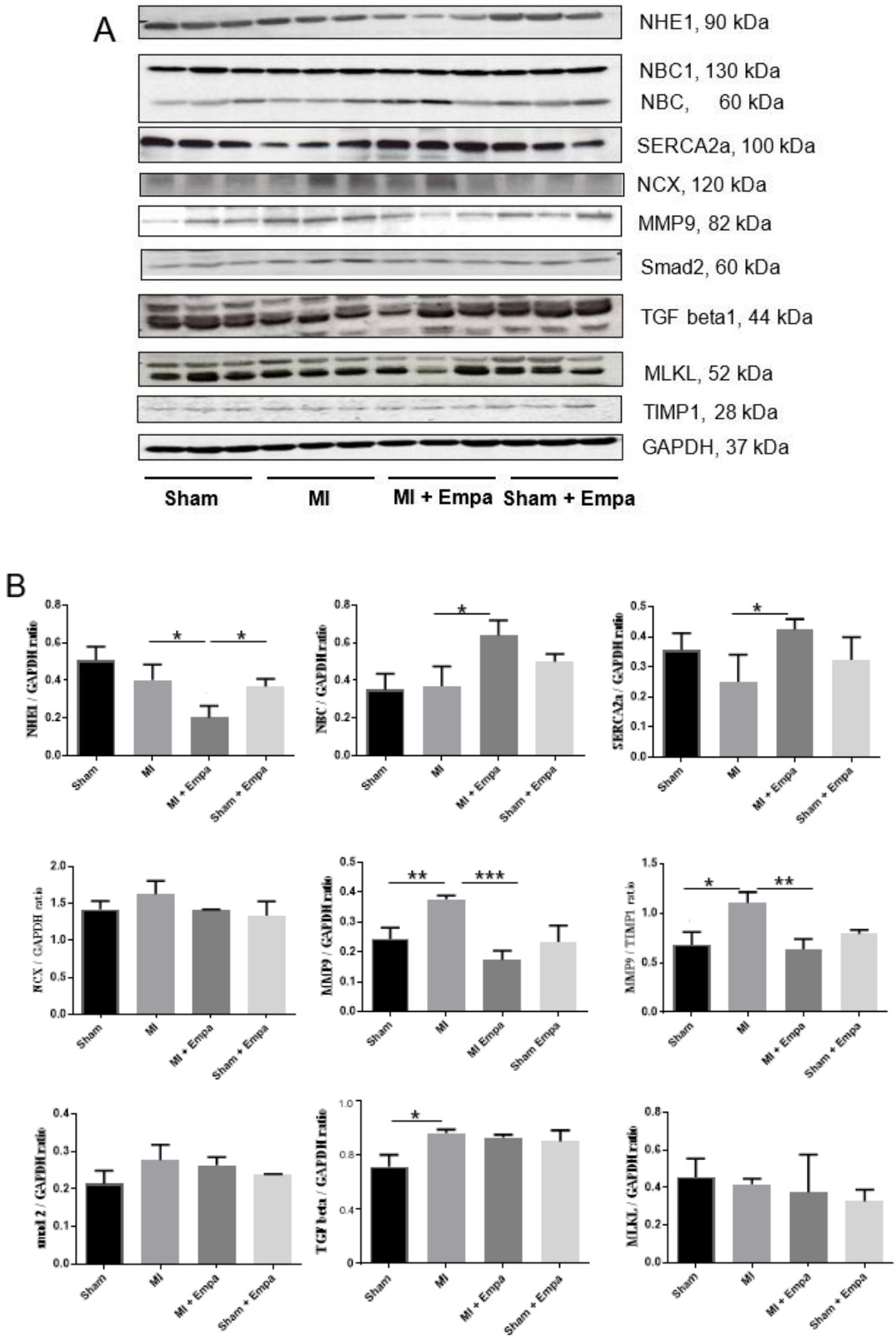

Figure 3. Molecular biological analysis of left ventricular 7 days after myocardial infarction. Western blot analysis of cardiac transporters (NHE1, NBC, NCX, SERCA2a), matrix metalloprotease 9 (MMP9), markers of fibrosis (smad, TGF-β1), marker of necroptosis (MLKL). (**A**) Representative Western blots: sham operation, MI vehicle, MI treated with Empa, sham operation treated with Empa. (**B**) Densitometric data of proteins are mean ± SEM (bars); * $P < 0.05$; ** $P < 0.01$; *** $P < 0.001$; two-tailed unpaired *t*-test.

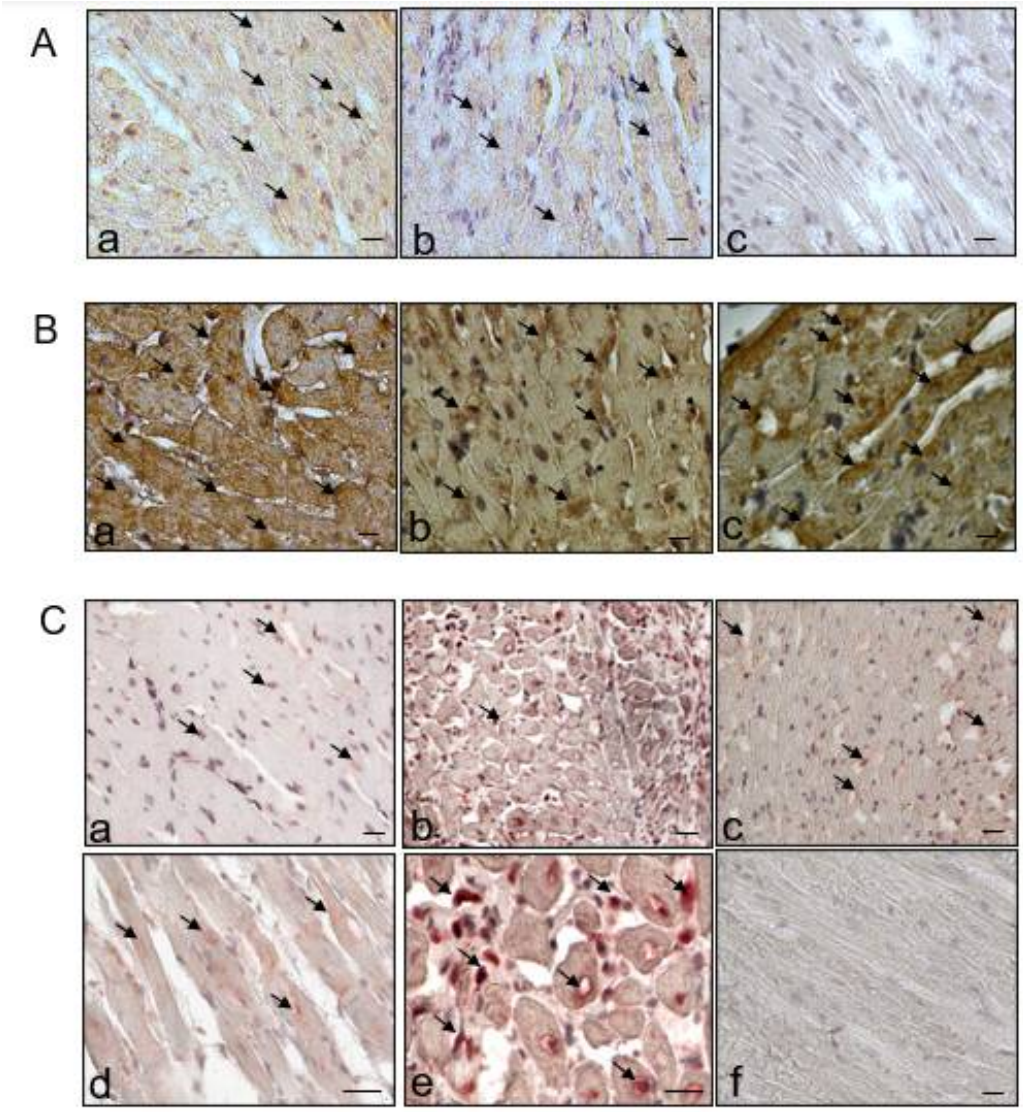

Figure 4. Cross-sections of the heart left ventricular, peri-infarct zone, immunohistological staining. (**A**) NHE1 (red stain), ×40; (**a**) MI vehicle; (**b**) MI treated with Empa; (**c**) negative control. (**B**) SERCA2a (brown stain), ×60; (**a**) sham operation; (**b**) MI vehicle; (**c**). MI treated with Empa. (**C**) MMP9 (red stain); (**a**) sham operation ×40; (**b**) MI vehicle, ×40; (**c**) MI treated with Empa, ×40 (**d**) MI vehicle ×60, MMP9 expression within cardiac myocytes; (**e**) MI vehicle ×60, MMP9 expression around the inflammatory cells and nuclei; (**f**) negative control. Scale 100 pixels.

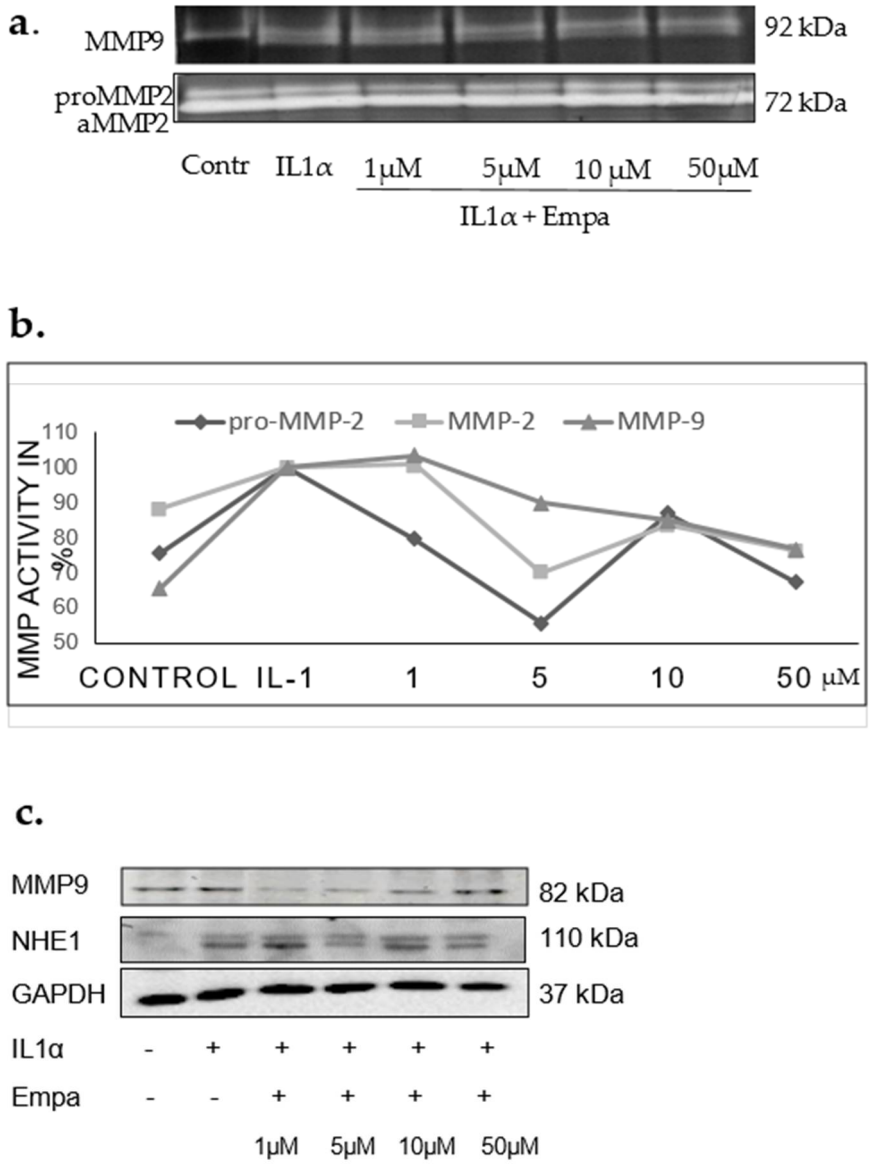

Figure 5. (**a**) Gelatin zymography, H9c2 cells, representative zymogram (**b**). Results from 3 experiments, 3 replicates; proMMP2, MMP2, MMP9 activity related to control after stimulation with IL1α and treatment with Empa 1, 5, 10, 50 μM. (**c**) Representative Western blots of MMP9, NHE1, GAPDH expression in H9c2 cells, 48 h after stimulation with IL1α.

2.4. Regulation of MMP2, MMP9, and TIMP1

In the left ventricle, an up-regulation of MMP9 post-MI (1.6-fold) was attenuated by Empa ($p < 0.001$) (Figure 3A,B). TIMP1 was not significantly regulated. Accordingly, the MMP9/TIMP1 ratio was regulated similarly to MMP9 (Figure 3B). In the peri-infarct zone, MMP9 was localized inside cardiomyocytes (Figure 4C(d)); around the nucleus (Figure 4C(e)); and co-localized with the inflammatory cells (Figure 4C(b,e)) and intramyocardial adipocytes. Less expression was found after Empa treatment (Figure 4C(c)).

In cardiac cell line H9c2, Empa decreased the activity of IL1α stimulated proMMP2, MMP2, and MMP9 compared to IL1α control (Figure 5a,b). The protein expression of MMP9 was also diminished by Empa (1–10 μM), although it was increased at a concentration of 50 μM (Figure 5). At the concentration of 1 μM, Empa prevented apoptosis, decreasing the apoptosis ratio by 25%.

2.5. Regulation of Fibrosis and Necroptosis

Post-MI increase of fibrotic markers TGF-beta1 (1.3-fold; $p < 0.05$) and smad2 (1.3-fold) expression was not modified by treatment (Figure 3A,B). MLKL, a marker of necroptosis, was also not regulated post-MI, although it was slightly decreased (1.4-fold) in Empa treated sham animals compared with sham (Figure 3A,B).

3. Discussion

SGLT2 inhibitors earned great attention from investigators due to the recently discovered pleiotropic cardioprotective effects. Besides favorable actions on the heart by treating diabetes [1,26], SGLT2 inhibitors also protected normoglycemic animals in heart failure models [7,8,10,11], myocardial infarction [13,14], and occlusion/reperfusion models [12]. Nevertheless, in clinical [4,5] and experimental [7,8,14] studies, there are controversial issues regarding systolic and diastolic heart function improvement. The mechanism of cardiac action is also not fully understood.

Our study showed that short-time application of Empa to healthy animals increased the ventricular systolic pressure, mean pressure, the max dP/dt, and maximal pressure in the aorta. Similarly, the application of Empa in a low dose in the sham group showed an increase in cardiac output, stroke volume, and fractional shortening. Thus, Empa improved the systolic heart function in non-diseased rats beyond modifying the heart rhythm.

Reduced global longitudinal strain (GLS) post-MI points to the favorable effect of Empa on the systolic function by early left ventricular remodeling. We could not demonstrate an improvement of the diastolic function; however, the diastolic parameter E/A tended to decrease after treatment.

Empa did not influence vascular parameters such as arterial augmentation index, maximal pressure in aorta (P2), and pulse pressure (Pp). Therefore, its favorable hemodynamic effects could be primarily attributed to improved cardiac contractility. These findings on the systolic function are in agreement with several recent studies [7,8,10,14].

An increase in the indices of force and the rate of change in variables of ventricular contraction (fractional shortening, stroke volume, and cardiac output) after Empa administration suggests a positive inotropic effect. Thus, increased contractility may reduce a mismatch between oxygen delivery to tissue and organ demand by cardiovascular pathology.

Blood pressure was not lowered by the treatment, and rather tended to increase in short-term experiments. This result is in agreement with a heart failure study in non-diabetic rats by Connelly et al. [15].

One-week treatment with a low dose of Empa induced a markable decrease in weight. The sham-treated group also showed the same results. This effect, probably due to the catabolic state [14,15] could be unfavorable by non-obese or post-MI subjects.

Positive inotropy is generally attributed to the cardiac actin-myosin cycle that depends on intracellular cAMP, calcium transients, or calcium-myosin activation. In this study, we focused on calcium transporters. Recently, Baartscheer et al. [32] discovered that the NHE1 blockade by Empa, independent from the SGLT2 receptor, decreased cytosolic sodium and calcium levels; and increased myocytes mitochondrial calcium concentration. Here, we provide in vivo evidence that Empa ameliorates an up-regulation of NHE1 expression in the left ventricular post-MI.

Nevertheless, we did not find a subsequent down-regulation of the NCX which is also an essential regulator of cardiac contractility independent of sarcoplasmic reticulum Ca^{2+} load [36]. Its increased activity promotes heart failure, cardiac ischemia, and arrhythmia [36].

Since sodium bicarbonate cotransporter 1 (NBCe1) also contributes to the control of intracellular pH in cardiomyocytes, we were interested in its regulation. The NBC membrane family proteins are responsible for 30% of Na+ influx into the cells during the recovery from acidosis [37]. The increase in Na+ is crucial for the heart because it decreases the driving force of the NCX leading to Ca^{2+} overload. Furthermore, NBC blockade reduces ischemic Na+ overload in isolated rat hearts [38]. In our study, in heart tissues, the NBC

130 kDa band that corresponds to the NBCe1 transporter was not regulated, although the 60 kDa form was up-regulated. Unfortunately, the results obtained in cell culture experiments as well in the other tissues provided differential expression muster. Therefore, further investigations on NBCe1 regulation by using another experimental approach would be required.

Current evidence suggests a cooperative action of NHE1 as an ion transporter and as a membrane scaffold in promoting the assembly of signaling complexes [41]. Interestingly, we found a down-regulation of MMP9 protein expression in the heart by Empa. This effect on MMP9 was confirmed in cultured cardiac cells in which Empa decreased the MMP9 activity. The expression of MMP9 is probably regulated by NHE1 while it creates an acidic environment that, in turn, activates proteolytic enzymes. This suggestion is in agreement with the study by Putney and Barber [42] who found that loss of NHE1 activity in mammalian fibroblasts decreased the MMP9 of the cells. Similarly, MMP9 processing was altered in cells expressing a defective NHE1 [39]. Since the expression of a native MMP9 inhibitor TIMP1, as well as TGF-beta1/smad2 regulation, were not modified in the present study, their impact in MMP9 regulation by Empa could be excluded. Notably, down-regulation of MMPs by Empa is of major importance because this effect could be relevant to other diseases including cancer.

Sarco/endoplasmic reticulum Ca^{2+}-ATPase (SERCA)2a is the primary cardiac isoform regulating intracellular Ca^{2+} homeostasis. Its increased expression improves myocardial contractility and Ca^{2+} handling [43]. Importantly, high mechanical stress is directly linked to SERCA2a down-regulation and slowing of relaxation [35]. In the post-MI model of the rat, regional diastolic dysfunction was linked to elevated wall stress adjacent to the infarction, resulting in down-regulation of SERCA, disrupted diastolic Ca^{2+} handling, and local slowing of relaxation [35].

In our study, SERCA2a expression in the left ventricular tissues adjusted to the scar was also decreased post-MI and its decrease was ameliorated by Empa. Notably, an increase in SERCA2a was accompanied by the down-regulation of MMP9. An interplay between SERCA2a and MMP9 has been previously shown in cardiomyocytes where ablation of MMP9 prevented contractile dysfunction by increasing SERCA2a and calcium transients [44]. Therefore, the favorable effect of Empa on cardiac contractility post-MI could be explained by the increased SERCA2a, where regulation seems to be interrelated with MMP9 and NHE1.

Therefore, Empa in low dose increases cardiac contractility in normoglycemic healthy rats and improves systolic heart function post-MI. These effects may be attributed to the up-regulation of SERCA2a and down-regulation of MMP9 and NHE1.

4. Materials and Methods

4.1. Ethics Statement

This study was carried out in strict accordance with the national and European guidelines for animal experiments with approval by the ethics commission of the regulatory authorities of the City of Berlin, Germany, the "Landesamt fuer Gesundheit und Soziales" (registration number G0128/17, 22 August 2017).

4.2. Animals

Male normotensive Wistar rats (6 weeks old; weight, 200 to 220 g; Charles River Laboratories Germany GmbH, Sulzfeld, Germany) were kept in an SPF (specific pathogen-free) barrier under standardized conditions with respect to temperature and humidity and were housed on a 12 h light/12 h dark cycle in groups of four animals with freely accessible food and water.

4.3. Experimental Protocol

The acute effect of Empa (1 mg/kg, in 0.5 mL NaCl, i.v. in the vena femoralis) on left ventricular (LV) pressure was examined in healthy animals under 1.5–2% isoflurane. The ventricular pressure was recorded over a time period of 30 min.

MI was induced by ligation of the proximal left anterior descending coronary artery as previously described [33]. The rats were randomly assigned to the following groups: Empa treatment (1 mg/kg daily p.o.) (n = 7), vehicle treatment (0.9% NaCl) (n = 8), and sham-operated controls (n = 6). Treatment was started 24 h after MI. Animals with ejection fraction <35% were excluded from the experiment before assignment to groups.

4.4. Analysis of Hemodynamic Parameters

Transthoracic Doppler echocardiography was performed preoperatively and on day 7 postoperatively in rats anesthetized with isoflurane (2%) with the use of the high-resolution imaging system Vevo 3100 (VisualSonics, Toronto, ON, Canada). Echocardiographic parameters are known to correlate with the heart structure and metabolic changes in rats [45].

The short axis and long axis were recorded in B- and M-Mode. The flow velocity of the mitral valve was calculated via Pulse Wave Doppler presented in 4-chamber view. All data were evaluated using the VevoLab software (Version 2.2.0, VisualSonics Inc., Toronto, ON, Canada) as previously described [46,47].

The invasive hemodynamic assessment was performed at the end of the study on day 7 using a fiber-optic pressure transducer catheter (Samba Sensors, Västra Frölunda, Sweden) and Chart5 software (Blood Pressure Module) for analysis as previously described [46]. Briefly, after anesthesia with isoflurane (2%), the catheter was inserted into the right carotid artery. After recording blood pressure and heart rate in the ascending aorta, the catheter was advanced into the left ventricle and the pressure-time indices (dP/dt_{min} and dP/dt_{max}) were recorded. Pulse wave analysis (PWA) was performed as previously described [48]. Diastolic pressure (Pd), pulse pressure (Pp), and systolic pressure (Ps) were determined and averaged on the central aortic pressure waveforms from at least 20 cardiac cycles.

4.5. Glucose Levels

Glucose levels were determined in rat serum and urine collected 7 days after MI by enzymatic photometric test using Glucose GOD FS kit (DiaSys Diagnostic Systems GmbH, Number 125509910021). Determination of glucose was based upon the Trinder technique, an oxidation reaction by glucose oxidase. Chinonimin was used as colorimetric indicator.

4.6. Immunoblotting Analysis

Protein preparation and Western blot analysis were carried out as described previously [49]. Immunoblotting was performed using NHE1 (Abbiotec, San Diego, CA, USA), NBC1 (Cohesion Bioscience, London, UK), NCX (Swant, Marly, Switzerland), SERCA2a (Dianova, Hamburg, Germany), MMP9 and GAPDH Ab (Abcam, Hiddenhausen, Germany), TIMP-1, TGF-beta1, Smad2 Ab (Santa Cruz Biotechnology Inc., Heidelberg, Germany), MLKL (Millipore, Merk, Darmstadt, Germany). GAPDH was used as a loading control. The antibodies dilution is presented in Supplementary Table S1. Immunoreactive bands were visualized by enhanced chemiluminescence (Amersham-Pharmacia, Freiburg, Germany) and quantified by densitometry with Scion Image software.

4.7. Immunohistochemistry

Paraffin-embedded cross-sections of the heart (4 µm) were stained and analyzed by quantitative morphometry (Biorevo BZ-9000, Keyence, Japan). Immunohistochemistry was performed using the avidin–biotin complex method according to the manufacturer's instructions (Vectastain ABC, Vector Laboratories, Burligame, CA, USA). Peroxidase activity was visualized by 3-amino-9-ethylcarbazole (AEC, Vector Laboratories, Burlingame, CA, USA) or 3,3'-diaminbenzidin (DAB) (Sigma-Aldrich Chemie, Darmstadt, Germany). The following primary antibodies were used: NHE1, MMP9, and SERCA2a. The dilution of the

first antibody was 1:200 incubated overnight at 4 °C. The second antibody was diluted 1:500 and incubated for 1 h at room temperature. The ABC reagent was prepared according to the protocol and given to the slides for 30 min. It binds with the second biotinylated antibody. The AEC substrate or the DAB combines with this complex and a color reaction occurs.

4.8. Cell Culture

Neonatal rat cardiomyocytes (H9c2 cell line, Sigma-Aldrich, Merk, Germany) were incubated for 10 h in high-glucose Dulbecco's modified Eagle's medium plus 10% fetal bovine serum and treated with 1 ng/mL recombinant interleukin 1α (IL1α) to induce cytokine expression and mimic the post-MI inflammatory response in the heart. Incubation was performed with or without co-incubation with 5, 10, 50 μM empagliflozin (Toronto Research Chemicals, Toronto, ON, Canada). Protein expression of NHE1 was evaluated by immunoblotting, and activities of MMP2 and MMP9 were analyzed with gelatin zymography as previously described [50].

4.9. Statistical Analysis

Results are expressed as mean ± SD. Multiple comparisons were analyzed using two-way repeated measures analysis of variance (ANOVA) followed by Bonferroni's multiple comparisons test. Two-group comparisons were analyzed by the 2-tailed Student unpaired *t*-test for independent samples. Differences were considered statistically significant at the value of $p < 0.05$. Statistical analysis was performed using GraphPad Prism 6 (GraphPad Software Inc., La Jolla, CA, USA).

5. Conclusions

In conclusion, short-term treatment with Empa in a low dose increased cardiac contractility in normoglycemic rats and improved systolic heart function in the early phase after myocardial infarction.

Empa administration did not alter arterial stiffness, blood pressure, markers of fibrosis, and necroptosis.

Cellular mechanisms that minimize cardiac damage by Empa include anti-proteolysis via the inhibition of MMP9, which is associated with decreased expression of NHE1, and prevention of apoptotic cell death.

Our study is of clinical relevance because it suggests that a low-dose treatment option with Empa may improve cardiovascular outcomes post-MI. Down-regulation of MMPs by Empa is of major importance because this effect could be relevant to many remodeling processes including cancer disease.

Supplementary Materials: The following are available online at https://www.mdpi.com/article/10.3390/ijms22115437/s1.

Author Contributions: J.G.: conception and design, performing animal experiments, collection and assembly of data, data analysis and interpretation; M.S., D.L., D.I.: collection and assembly of data; B.G., Y.S.: cell culture experiments, data analysis; S.O., A.K.: conception and design, data analysis and interpretation; U.K.: administrative support and advising on manuscript writing; E.K.: conception and design, provision of study material, collection and assembly of data, data analysis and interpretation, manuscript writing, final approvement of manuscript. All authors have read and agreed to the published version of the manuscript.

Funding: This work was funded by Charité Universitätsmedizin Berlin, Germany and Saint-Petersburg State Chemical-Pharmaceutical University, Saint Petersburg, Russia (AAAA-B20-220022590079-8).

Institutional Review Board Statement: The study was conducted according to the guidelines of the Declaration of Helsinki, and approved by the Ethics Committee of the regulatory authorities of the City of Berlin, Germany, the "Landesamt fuer Gesundheit und Soziales" (registration number G0128/17).

Informed Consent Statement: Not applicable.

Data Availability Statement: The data presented in this study are available on request from the corresponding author.

Conflicts of Interest: Ulrich Kintscher received research grants/speaker honoraria from Bayer. UK received speaker honoraria from Berlin Chemie, Boehringer Ingelheim, Daiichi Sankyo, Novartis, Sanofi, Servier, and participated in advisory boards of Berlin Chemie, Boehringer Ingelheim, Novartis, and Sanofi. The funders had no role in the design of the study; in the collection, analyses, or interpretation of data; in the writing of the manuscript, or in the decision to publish the results.

Abbreviations

EF	ejection fraction
FS	fractional shortening
GLS	Global Longitudinal Strain
IL-1α	Interleukin 1 alpha
max dP/dt	maximal rate of rise of left ventricular pressure
min dP/dt	minimal rate of rise of left ventricular pressure
MLKL	mixed lineage kinase domain-like
MMP	matrix metalloproteinase
NBC	sodium bicarbonate cotransporter 1
NCX	Na^+/Ca^{2+} exchanger
NHE1	sodium hydrogen exchanger 1
SERCA2a	Sarco(endo)plasmic reticulum Ca2-ATPase
SGLT2	Selective sodium-glucose cotransporter 2
SV	stroke volume
TGF β1	transforming growth factor beta1
TIMP1	tissue inhibitor of matrix metalloproteinase 1

References

1. Zinman, B.; Lachin, J.M.; Inzucchi, S.E. Empagliflozin, cardiovascular outcomes, and mortality in Type 2 Diabetes. *N. Engl. J. Med.* **2016**, *374*, 1094. [CrossRef] [PubMed]
2. Sinha, B.; Ghosal, S. Sodium-glucose cotransporter-2 inhibitors (SGLT-2i) reduce hospitalization for heart failure only and have no effect on atherosclerotic cardiovascular events: A meta-analysis. *Diabetes Ther.* **2019**, *10*, 891–899. [CrossRef] [PubMed]
3. Mahaffey, K.W.; Neal, B.; Perkovic, V.; de Zeeuw, D.; Fulcher, G.; Erondu, N.; Shaw, W.; Fabbrini, E.; Sun, T.; Li, Q.; et al. Canagliflozin for primary and secondary prevention of cardiovascular events: Results from the canvas program (canagliflozin cardiovascular assessment study). *Circulation* **2018**, *137*, 323–334. [CrossRef] [PubMed]
4. Wiviott, S.D.; Raz, I.; Bonaca, M.P.; Mosenzon, O.; Kato, E.T.; Cahn, A.; Silverman, M.G.; Zelniker, T.A.; Kuder, J.F.; Murphy, S.A.; et al. Dapagliflozin and Cardiovascular Outcomes in Type 2 Diabetes. *N. Engl. J. Med.* **2019**, *380*, 347–357. [CrossRef] [PubMed]
5. Norhammar, A.; Bodegård, J.; Nyström, T.; Thuresson, M.; Nathanson, D.; Eriksson, J.W. Dapagliflozin and cardiovascular mortality and disease outcomes in a population with type 2 diabetes similar to that of the DECLARE-TIMI 58 trial: A nationwide observational study. *Diabetes Obes. Metabol.* **2019**, *21*, 1136–1145. [CrossRef] [PubMed]
6. Fathi, A.; Vickneson, K.; Singh, J.S. SGLT2-inhibitors; more than just glycosuria and diuresis. *Heart Fail Rev.* **2021**, *26*, 623–642. [CrossRef] [PubMed]
7. Byrne, N.J.; Parajuli, N.; Levasseur, J.L.; Boisvenue, J.; Beker, D.L.; Masson, G.; Fedak, P.W.; Verma, S.; Dyck, J.R. Empagliflozin prevents worsening of cardiac function in an experimental model of pressure overload-induced heart failure. *JACC Basic Transl. Sci.* **2017**, *2*, 347–354. [CrossRef] [PubMed]
8. Connelly, K.A.; Zhang, Y.; Visram, A.; Advani, A.; Batchu, S.N.; Desjardins, J.F.; Thai, K.; Gilbert, R.E. Empagliflozin improves diastolic function in a nondiabetic rodent model of heart failure with preserved ejection fraction. *JACC Basic Transl. Sci.* **2019**, *4*, 27–37. [CrossRef] [PubMed]
9. Pabel, S.; Wagner, S.; Bollenberg, H.; Bengel, P.; Kovacs, A.; Schach, C.; Tirilomis, P.; Mustroph, J.; Renner, A.; Gummert, J.; et al. Empagliflozin directly improves diastolic function in human heart failure. *Eur. J. Heart Fail.* **2018**, *20*, 1690–1700. [CrossRef] [PubMed]
10. Santos-Gallego, C.G.; Requena-Ibanez, J.A.; San Antonio, R.; Ishikawa, K.; Watanabe, S.; Picatoste, B.; Flores, E.; Garcia-Ropero, A.; Sanz, J.; Hajjar, R.J.; et al. Empagliflozin ameliorates adverse left ventricular remodeling in nondiabetic heart failure by enhancing myocardial energetics. *J. Am. Coll. Cardiol.* **2019**, *73*, 1931–1944. [CrossRef]
11. Krasnova, M.; Kulikov, A.; Okovityi, S.; Ivkin, D.; Karpov, A.; Kaschina, E.; Smirnov, A. Comparative efficacy of empagliflozin and drugs of baseline therapy in post-infarct heart failure in normoglycemic rats. *Naunyn Schmiedebergs Arch. Pharmacol.* **2020**, *393*, 1649–1658. [CrossRef] [PubMed]

12. Lim, V.G.; Bell, R.M.; Arjun, S.; Kolatsi-Joannou, M.; Long, D.A.; Yellon, D.M. SGLT2 inhibitor, canagliflozin, attenuates myocardial infarction in the diabetic and nondiabetic heart. *JACC Basic Transl Sci.* **2019**, *4*, 15–26. [CrossRef] [PubMed]
13. Oshima, H.; Miki, T.; Kuno, A.; Mizuno, M.; Sato, T.; Tanno, M.; Yano, T.; Nakata, K.; Kimura, Y.; Abe, K.; et al. Empagliflozin, an SGLT2 inhibitor, reduced the mortality rate after acute myocardial infarction with modification of cardiac metabolomes and antioxidants in diabetic rats. *J. Pharmacol. Exp. Ther.* **2019**, *368*, 524–534. [CrossRef] [PubMed]
14. Yurista, S.R.; Silljé, H.H.; Oberdorf-Maass, S.U.; Schouten, E.M.; Pavez Giani, M.G.; Hillebrands, J.L.; van Goor, H.; van Veldhuisen, D.J.; de Boer, R.A.; Westenbrink, B.D. Sodium-glucose co-transporter 2 inhibition with empagliflozin improves cardiac function in non-diabetic rats with left ventricular dysfunction after myocardial infarction. *Eur. J. Heart Fail.* **2019**, *21*, 862–873. [CrossRef] [PubMed]
15. Connelly, K.A.; Zhang, Y.; Desjardins, J.F.; Nghiem, L.; Visram, A.; Batchu, S.N.; Yerra, V.G.; Kabir, G.; Thai, K.; Advani, A.; et al. Load-independent effects of empagliflozin contribute to improved cardiac function in experimental heart failure with reduced ejection fraction. *Cardiovasc. Diabetol.* **2020**, *19*, 13. [CrossRef] [PubMed]
16. Liu, Y.; Wu, M.; Xu, J.; Xu, B.; Kang, L. Empagliflozin prevents from early cardiac injury post myocardial infarction in non-diabetic mice. *Eur. J. Pharm. Sci.* **2021**, *161*, 105788. [CrossRef] [PubMed]
17. Sayour, A.A.; Celeng, C.; Oláh, A.; Ruppert, M.; Merkely, B.; Radovits, T. Sodium-glucose cotransporter 2 inhibitors reduce myocardial infarct size in preclinical animal models of myocardial ischaemia-reperfusion injury: A meta-analysis. *Diabetologia* **2021**, *64*, 737–748. [CrossRef] [PubMed]
18. Xue, M.; Li, T.; Wang, Y.; Chang, Y.; Cheng, Y.; Lu, Y.; Liu, X.; Xu, L.; Li, X.; Yu, X.; et al. Empagliflozin prevents cardiomyopathy via sGC-cGMP-PKG pathway in type 2 diabetes mice. *Clin. Sci.* **2019**, *133*, 1705–1720. [CrossRef] [PubMed]
19. Azam, M.A.; Chakraborty, P.; Si, D.; Du, B.; Massé, S.; Lai, P.F.; Ha, A.C.; Nanthakumar, K. Anti-arrhythmic and inotropic effects of empagliflozin following myocardial ischemia. *Life Sci.* **2021**, *1*, 119440. [CrossRef]
20. Peng, X.; Li, L.; Zhang, M.; Zhao, Q.; Wu, K.; Bai, R.; Ruan, Y.; Liu, N. Sodium-glucose cotransporter 2 inhibitors potentially prevent atrial fibrillation by ameliorating ion handling and mitochondrial dysfunction. *Front. Physiol.* **2020**, *4*, 912. [CrossRef]
21. Wright, E.M.; Loo, D.D.; Hirayama, B.A. Biology of human sodium glucose transporters. *Physiol. Rev.* **2011**, *91*, 733–794. [CrossRef] [PubMed]
22. Vrhovac, I.; Eror, D.B.; Klessen, D.; Burger, C.; Breljak, D.; Kraus, O.; Radović, N.; Jadrijević, S.; Aleksic, I.; Walles, T.; et al. Localizations of Na(+)-D-glucose cotransporters SGLT1 and SGLT2 in human kidney and of SGLT1 in human small intestine, liver, lung, and heart. *Pflug. Arch.* **2015**, *467*, 1881–1898. [CrossRef] [PubMed]
23. Banerjee, S.K.; McGaffin, K.R.; Pastor-Soler, N.M.; Ahmad, F. SGLT1 is a novel cardiac glucose transporter that is perturbed in disease states. *Cardiovasc. Res.* **2009**, *84*, 111–118. [CrossRef] [PubMed]
24. Filippatos, T.D.; Liontos, A.; Papakitsou, I.; Elisaf, M.S. SGLT2 inhibitors and cardioprotection: A matter of debate and multiple hypotheses. *Postgrad. Med.* **2019**, *131*, 82–88. [CrossRef] [PubMed]
25. Chilton, R.; Tikkanen, I.; Cannon, C.P.; Crowe, S.; Woerle, H.J.; Broedl, U.C.; Johansen, O.E. Effects of empagliflozin on blood pressure and markers of arterial stiffness and vascular resistance in patients with type 2 diabetes. *Diabetes Obes. Metabol.* **2015**, *17*, 1180–1193. [CrossRef] [PubMed]
26. Tikkanen, I.; Narko, K.; Zeller, C.; Green, A.; Salsali, A.; Broedl, U.C.; Woerle, H.J. Empagliflozin reduces blood pressure in patients with type 2 diabetes and hypertension. *Diabetes Care* **2015**, *38*, 420–428. [CrossRef] [PubMed]
27. Nikolic, M.; Zivkovic, V.; Jovic, J.J.; Sretenovic, J.; Davidovic, G.; Simovic, S.; Djokovic, D.; Muric, N.; Bolevich, S.; Jakovljevic, V. SGLT2 inhibitors: A focus on cardiac benefits and potential mechanisms. *Heart Fail Rev.* **2021**. [CrossRef] [PubMed]
28. Verma, S.; Rawat, S.; Ho, K.L.; Wagg, C.S.; Zhang, L.; Teoh, H.; Dyck, J.E.; Uddin, G.M.; Oudit, G.Y.; Mayoux, E.; et al. Empagliflozin increases cardiac energy production in diabetes: Novel translational insights into the heart failure benefits of SGLT2 Inhibitors. *JACC Basic Transl. Sci.* **2018**, *3*, 575–587. [CrossRef] [PubMed]
29. Byrne, N.J.; Matsumura, N.; Maayah, Z.H.; Ferdaoussi, M.; Takahara, S.; Darwesh, A.M.; Levasseur, J.L.; Jahng, J.W.; Vos, D.; Parajuli, N.; et al. Empagliflozin blunts worsening cardiac dysfunction associated with reduced NLRP3 (nucleotide-binding domain-like receptor protein 3) inflammasome activation in heart failure. *Circ. Heart Fail.* **2020**, *13*, e006277. [CrossRef]
30. Li, X.; Lu, Q.; Qiu, Y.; do Carmo, J.M.; Wang, Z.; da Silva, A.A.; Mouton, A.; Omoto, A.C.; Hall, M.E.; Li, J.; et al. Direct cardiac actions of the sodium glucose co-transporter 2 inhibitor empagliflozin improve myocardial oxidative phosphorylation and attenuate pressure-overload heart failure. *J. Am. Heart Assoc.* **2021**, *10*, e018298. [CrossRef] [PubMed]
31. Mustroph, J.; Wagemann, O.; Lücht, C.M.; Trum, M.; Hammer, K.P.; Sag, C.M.; Lebek, S.; Tarnowski, D.; Reinders, J.; Perbellini, F.; et al. Empagliflozin reduces Ca/calmodulin-dependent kinase II activity in isolated ventricular cardiomyocytes. *ESC Heart Fail.* **2018**, *5*, 642–648. [CrossRef] [PubMed]
32. Baartscheer, A.; Schumacher, C.A.; Wüst, R.C.; Fiolet, J.W.; Stienen, G.J.; Coronel, R.; Zuurbier, C.J. Empagliflozin decreases myocardial cytoplasmic Na. *Diabetologia* **2017**, *60*, 568–573. [CrossRef] [PubMed]
33. Uthman, L.; Nederlof, R.; Eerbeek, O.; Baartscheer, A.; Schumacher, C.; Buchholtz, N.; Hollmann, M.W.; Coronel, R.; Weber, N.C.; Zuurbier, C.J. Delayed ischaemic contracture onset by empagliflozin associates with NHE1 inhibition and is dependent on insulin in isolated mouse hearts. *Cardiovasc. Res.* **2019**, *115*, 1533–1545. [CrossRef] [PubMed]
34. Neef, S.; Maier, L.S. Novel aspects of excitation-contraction coupling in heart failure. *Basic Res. Cardiol.* **2013**, *108*, 360. [CrossRef] [PubMed]

35. Røe, Å.T.; Ruud, M.; Espe, E.K.; Manfra, O.; Longobardi, S.; Aronsen, J.M.; Nordén, E.S.; Husebye, T.; Kolstad, T.R.S.; Cataliotti, A.; et al. Regional diastolic dysfunction in post-infarction heart failure: Role of local mechanical load and SERCA expression. *Cardiovasc. Res.* **2019**, *115*, 752–764. [CrossRef] [PubMed]
36. Ottolia, M.; Torres, N.; Bridge, J.H.; Philipson, K.D.; Goldhaber, J.I. Na/Ca exchange and contraction of the heart. *J. Mol. Cell. Cardiol.* **2013**, *61*, 28–33. [CrossRef] [PubMed]
37. Bernardo, A.A.; Bernardo, C.M.; Espiritu, D.J.; Arruda, J.A. The sodium bicarbonate cotransporter: Structure, function, and regulation. *Semin. Nephrol.* **2006**, *26*, 352–360. [CrossRef] [PubMed]
38. Ten Hove, M.; Nederhoff, M.G.; van Echteld, C.J. Relative contributions of Na+/H+ exchange and Na+/HCO3- cotransport to ischemic Nai+ overload in isolated rat hearts. *Am. J. Physiol. Heart Circ. Physiol.* **2005**, *288*, H287–H292. [CrossRef] [PubMed]
39. Taves, J.; Rastedt, D.; Canine, J.; Mork, D.; Wallert, M.A.; Provost, J.J. Sodium hydrogen exchanger and phospholipase D are required for alpha1-adrenergic receptor stimulation of metalloproteinase-9 and cellular invasion in CCL39 fibroblasts. *Arch. Biochem. Biophys.* **2008**, *477*, 60–66. [CrossRef]
40. Yang, C.C.; Chen, Y.T.; Wallace, C.G.; Chen, K.H.; Cheng, B.C.; Sung, P.H.; Li, Y.C.; Ko, S.F.; Chang, H.W.; Yip, H.K. Early administration of empagliflozin preserved heart function in cardiorenal syndrome in rat. *Biomed. Pharmacother.* **2019**, *109*, 658–670. [CrossRef]
41. Baumgartner, M.; Patel, H.; Barber, D.L. Na(+)/H(+) exchanger NHE1 as plasma membrane scaffold in the assembly of signaling complexes. *Am. J. Physiol. Cell. Physiol.* **2004**, *287*, C844–C850. [CrossRef] [PubMed]
42. Putney, L.K.; Barber, D.L. Expression profile of genes regulated by activity of the Na-H exchanger NHE1. *BMC Genom.* **2004**, *5*, 46. [CrossRef] [PubMed]
43. He, H.; Giordano, F.J.; Hilal-Dandan, R.; Choi, D.J.; Rockman, H.A.; McDonough, P.M.; Bluhm, W.F.; Meyer, M.; Sayen, M.R.; Swanson, E.; et al. Overexpression of the rat sarcoplasmic reticulum Ca2+ ATPase gene in the heart of transgenic mice accelerates calcium transients and cardiac relaxation. *J. Clin. Investig.* **1997**, *100*, 380–389. [CrossRef] [PubMed]
44. Prathipati, P.; Metreveli, N.; Nandi, S.S.; Tyagi, S.C.; Mishra, P.K. Ablation of matrix metalloproteinase-9 prevents cardiomyocytes contractile dysfunction in diabetics. *Front. Physiol.* **2016**, *7*, 93. [CrossRef] [PubMed]
45. Pop, C.; Berce, C.; Ghibu, S.; Pop, A.; Kiss, B.; Irimie, A.; Popa, Ș.T.; Cismaru, G.; Loghin, F.; An, M.Ș. Validation and characterization of a heart failure animal model. *Farmacia* **2016**, *64*, 435–443.
46. Kaschina, E.; Grzesiak, A.; Li, J.; Foryst-Ludwig, A.; Timm, M.; Rompe, F.; Sommerfeld, M.; Kemnitz, U.R.; Curato, C.; Namsolleck, P.; et al. Angiotensin II type 2 receptor stimulation: A novel option of therapeutic interference with the renin-angiotensin system in myocardial infarction? *Circulation* **2008**, *118*, 2523–2532. [CrossRef] [PubMed]
47. Beyhoff, N.; Lohr, D.; Foryst-Ludwig, A.; Klopfleisch, R.; Brix, S.; Grune, J.; Thiele, A.; Erfinanda, L.; Tabuchi, A.; Kuebler, W.M.; et al. Characterization of myocardial microstructure and function in an experimental model of isolated subendocardial damage. *Hypertension* **2019**, *74*, 295–304. [CrossRef] [PubMed]
48. Slavic, S.; Lauer, D.; Sommerfeld, M.; Kemnitz, U.R.; Grzesiak, A.; Trappiel, M.; Thöne-Reineke, C.; Baulmann, J.; Paulis, L.; Kappert, K.; et al. Cannabinoid receptor 1 inhibition improves cardiac function and remodelling after myocardial infarction and in experimental metabolic syndrome. *J. Mol. Med.* **2013**, *91*, 811–823. [CrossRef] [PubMed]
49. Lauer, D.; Slavic, S.; Sommerfeld, M.; Thöne-Reineke, C.; Sharkovska, Y.; Hallberg, A.; Dahlöf, B.; Kintscher, U.; Unger, T.; Steckelings, U.M.; et al. Angiotensin type 2 receptor stimulation ameliorates left ventricular fibrosis and dysfunction via regulation of tissue inhibitor of matrix metalloproteinase 1/matrix metalloproteinase 9 axis and transforming growth factor β1 in the rat heart. *Hypertension* **2014**, *63*, e60–e67. [CrossRef] [PubMed]
50. Vosgerau, U.; Lauer, D.; Unger, T.; Kaschina, E. Cleaved high molecular weight kininogen, a novel factor in the regulation of matrix metalloproteinases in vascular smooth muscle cells. *Biochem. Pharmacol.* **2010**, *79*, 172–179. [CrossRef] [PubMed]